

# Nuclear Magnetic Resonance of High-Spin Ferric Hemoproteins. Assignment of Proton Resonances in Met-Aquo Myoglobins Using Deuterium-Labeled Hemes

Gerd N. La Mar,\* David L. Budd, Kevin M. Smith,\* and Kevin C. Langry

Contribution from the Department of Chemistry, University of California, Davis, California 95616. Received June 11, 1979

**Abstract:** The high-field  $^1\text{H}$  NMR spectra of sperm whale high-spin ( $S = 5/2$ ) met-aquo myoglobin reconstituted with various specifically deuterated protohemes and deuterohemes are shown to lead to the resolution of 17, and the unambiguous assignment of 12, of the 22 possible heme resonances in the native protein. Two nonheme paramagnetically shifted methyl peaks are assigned to the distal valine E11. The heme methyl shift pattern is the same as in models, but reflects a much greater rhombic or in-plane asymmetry. The resonance positions of the meso and pyrrole protons confirm the presence of coordinated water and suggest that these peaks may be useful in probing the occupation of the sixth site in high-spin hemoproteins. The deviations from Curie law of vinyl and probable propionate group resonances are interpreted in terms of temperature-dependent orientations of these conformationally flexible side chains.

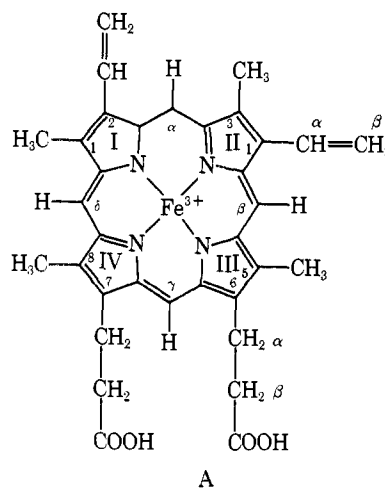
## Introduction

Concentrated efforts during the past decade on the  $^1\text{H}$  NMR studies of paramagnetic hemoproteins<sup>1-3</sup> have improved significantly our understanding of the structure-function relationships of hemoproteins in general.<sup>4</sup> Owing largely to the narrower resonance lines and the concomitant better sensitivity, the early focus was on low-spin ferric systems, although the biological relevance of the high-spin ferrous forms quickly led to numerous successful NMR studies of deoxyhemoglobins.<sup>1-4</sup> Reports on high-spin ferric hemoproteins, however, have been much less frequent,<sup>5-8</sup> probably because of the widespread belief that their broader lines necessarily lead to less well-resolved or less informative NMR spectra.

There are, however, compelling reasons for characterizing in detail the NMR spectra of high-spin ferric hemoproteins and exploring their information content. Firstly, there is available considerable structural information on met-aquo hemoglobins<sup>9</sup> and myoglobins<sup>10</sup> which could provide a basis for interpreting their NMR data, and there are several important hemoproteins, such as peroxidases,<sup>11</sup> catalases,<sup>12</sup> oxygenases,<sup>13</sup> and some ferricytochromes,<sup>14</sup> which contain high-spin iron(III) in their biologically active forms. Secondly, although high-spin ferric hemoprotein resonances may be much broader than for other oxidation/spin states,<sup>1-3,5-8</sup> the isotropic or hyperfine shifts are also much larger, and studies on models<sup>15-17</sup> suggest that perhaps many more heme resonances could be resolved in the ferric high-spin than in other forms of hemoproteins. The resolution of as many heme resonances as possible is critical to the evaluation of differential protein perturbations over the heme.

In order to assess the information content on a quantitative basis, not only must individual resonances be resolved, but they must also be assigned unambiguously to each functional group on the heme. Although early NMR work on hemoproteins emphasized empirical use of the paramagnetically shifted peaks of tentatively assigned resonances,<sup>1,2</sup> the recent introduction of isotopically methyl-labeled hemes provided a quantitative basis for interpreting the heme methyl shifts.<sup>3,17-20</sup> The first unambiguous heme methyl assignment<sup>18</sup> already indicated the problems encountered in proposing complex though reasonable interpretations<sup>21</sup> based on assumed assignments. Since this initial study,<sup>18</sup> unambiguous methyl peak assignments in low-spin ferric proteins have been shown to lead to valuable information on vinyl-group orientation and oscillatory mobility,<sup>22,23</sup> as well as to a method for determining the orientation<sup>19</sup> of the porphyrin within the heme pocket of an intact hemoprotein.

In this study we extend our strategy of deuterium labeling of hemin<sup>3,17,19,20</sup> (A) to effect as many as possible of the peak



assignments required for structural interpretation of the  $^1\text{H}$  NMR spectra of high-spin ferric hemoproteins. The purpose of this study is twofold. On the one hand, we wish to compare the utility of the NMR data for structural analysis in the different oxidation/spin states<sup>7,18,24</sup> of a given protein. Of particular interest is the role of the heme-apoprotein interactions in inducing rhombic or in-plane asymmetry in the heme, as monitored by the spread of the heme methyl shifts.<sup>3,17,19</sup> To this end we have selected sperm whale met-aquo myoglobin for this initial study, since NMR spectra in other states have been analyzed<sup>3,18,19,24</sup> and high-quality X-ray crystallographic data on this form<sup>10</sup> as well as other forms of this protein<sup>25,26</sup> are available. On the other hand, met-aquo myoglobin can serve as a model for the interesting class of heme peroxidases<sup>11,27</sup> about which considerably less structural detail is available, but whose proton spectra of the high-spin ferric resting enzyme<sup>28</sup> are sensitive to structural perturbations which can also be effected in myoglobin.<sup>29</sup> Moreover, met-aquo myoglobin may provide a test for specialized structural probes suggested based on studies on model complexes<sup>15-17,30</sup> such as the ability to infer from heme hyperfine shift pattern whether the sixth position on the iron is vacant.

## Experimental Section

Sperm whale myoglobin was purchased as a lyophilized, salt-free powder from Sigma. The  $^2\text{H}_2\text{O}$  (99.8%  $^2\text{H}$ ) was obtained from Bio-Rad. Protohemin, deuterium labeled at methyl-1 (~40%  $^2\text{H}$ ) and

methyl-3 (~60%  $^2\text{H}$ ), [1,3-( $\text{C}^2\text{H}_3$ ) $_2$ ]hemin (this compound also has the 6,7- $\text{H}_\beta$  approximately 80% deuterated), methyl-1 (~65%  $^2\text{H}$ ) and methyl-5 (~90%  $^2\text{H}$ ), [1,5-( $\text{C}^2\text{H}_3$ ) $_2$ ]hemin, the  $\alpha$  position of vinyl-2 and -4 (>90%  $^2\text{H}$ ), [2,4-( $^2\text{H}_\alpha$ ) $_2$ ]hemin, and both  $\beta$  positions of vinyl-2 and -4 (~90%  $^2\text{H}$ ), [2,4-( $^2\text{H}_\beta$ ) $_4$ ]hemin are the same material reported in detail previously.<sup>17,20</sup> Deuterohemin, A with 2- and 4-vinyls replaced by protons, was prepared from commercial hemin (Sigma) by standard procedures.<sup>31</sup> Two new deuterated hemins were prepared as follows.

**$\alpha,\beta,\gamma,\delta$ -meso-Tetradeterioprotophemin, [ $\alpha,\beta,\gamma,\delta$ -( $^2\text{H}$ ) $_4$ ]Hemin.** To 300 mg of protoporphyrin IX dimethyl ester was added a solution of hexapyridylmagnesium diiodide (prepared<sup>32</sup> from 1 g of iodine and 300 mg of magnesium) in 25 mL of pyridine and 4 mL of  $\text{CH}_3\text{O}^2\text{H}$ . After refluxing at 120 °C under nitrogen for 48 h the mixture was diluted with methylene chloride and washed once with water and then with 2 N hydrochloric acid and water again. The organic phase was evaporated to dryness and the red residue was treated in methylene chloride/methanol with excess ethereal diazomethane. After evaporation, the product was chromatographed on neutral alumina [Brockmann grade III, elution with toluene/methylene chloride (3:7)] and the appropriate fractions were crystallized from methylene chloride/*n*-hexane to give 160 mg (53%) of protoporphyrin IX dimethyl ester. Iron was inserted using the ferrous sulfate/pyridine/acetic acid method<sup>33</sup> and hydrolysis was accomplished by treatment with 1% KOH/4%  $\text{H}_2\text{O}$ /95%  $\text{CH}_3\text{OH}$  at 70 °C during 10 h.<sup>34</sup> The  $^1\text{H}$  NMR spectrum of the resulting dicyanoferric hemin in  $\text{C}^2\text{H}_3\text{O}^2\text{H}$  was identical with that reported<sup>20</sup> for unlabeled complex except that the assigned meso signals were approximately 80% deuterated.

**2,4-Dideuteriodeteroheemin, [2,4-( $^2\text{H}$ ) $_2$ ]Deuterohemin.** A sample of [( $^2\text{H}$ ) $_5$ ]resorcinol was prepared by stirring 5.5 g of resorcinol with 11 g of  $^2\text{H}_2\text{O}$  containing 2 mL of 20%  $^2\text{HCl}$  in  $^2\text{H}_2\text{O}$  overnight. The mixture was evaporated to dryness and the procedure was repeated once more. The resulting [( $^2\text{H}$ ) $_5$ ]resorcinol (1.20 g) and 295 mg of hemin were ground together and then fused under nitrogen at 160 °C for 45 min. After cooling to a paste the residue was triturated with 25 mL of ether and then the mixture was filtered and the precipitate was washed with ether until the filtrate was colorless. The brown solid was dissolved in 5 mL of pyridine and this was diluted with 100 mL of dry methanol. Ferrous sulfate (3 g) was added and, after chilling in an ice bath, the stirred solution was treated with a stream of HCl gas during 10 min. (The progress of this demetalation was monitored by spectrophotometry.) The solution was diluted with 150 mL of methylene chloride in 150 g of ice and the organic phase was collected. After back-extraction of the aqueous phase the combined organic layers were washed with water until neutral. The solution was evaporated to dryness and the residue was chromatographed on neutral alumina (Brockmann grade III, elution with methylene chloride). The product was crystallized from methanol/methylene chloride to give 188 mg (70%) of deuteroporphyrin IX dimethyl ester.  $^1\text{H}$  NMR analysis in  $\text{C}^2\text{HCl}_3$  indicated >90% deuteration at the 2 and 4 positions as well as partial deuteration at the meso positions. Iron was inserted into this sample using the ferrous sulfate/pyridine/acetic acid method<sup>33</sup> and the esters were hydrolyzed using 1% KOH/4%  $\text{H}_2\text{O}$ /95%  $\text{CH}_3\text{OH}$  at 70 °C during 10 h.<sup>34</sup> The  $^1\text{H}$  NMR spectrum of the resulting dicyanoferric hemin in  $\text{C}^2\text{H}_3\text{O}^2\text{H}$  was identical with that reported<sup>20</sup> for unlabeled complex except for the absence of the assigned 2 and 4 protons and reduced intensity of the meso signals.

Solutions of met-aquo myoglobin (metMbH $_2\text{O}$ ) were prepared by dissolving the myoglobin (1–2 mM) in 99.7%  $^2\text{H}_2\text{O}$  0.2 M in NaCl, and centrifuging to remove precipitate. The solution was converted completely to the met form by the addition of a twofold excess of ferricyanide, removing the ions by passing the solution over a Sephadex G-25 column equilibrated with 0.2 M NaCl, and eluting with the same solution. Apo-myoglobin was prepared by the method of Teale<sup>35</sup> and reconstituted with the appropriately deuterium-labeled or modified hemins as described by La Mar et al.<sup>19</sup> The resulting solutions were concentrated to 1–2 mM in heme by ultrafiltration. The pH (uncorrected) was adjusted to 6.2 using 0.1 M  $^2\text{HCl}$  and is therefore referred to as p $^2\text{H}$ . At p $^2\text{H}$  6.2, met-myoglobin is wholly in the met-aquo form,<sup>7</sup> i.e., met-Mb $^2\text{H}_2\text{O}$ .

$^1\text{H}$  NMR spectra were recorded on Nicolet NT-200 and NT-360 FT NMR spectrometers operating at 200 and 360 MHz, respectively. Typical spectra consisted of collecting 1000–10 000 transients using 8K points over 25–40 kHz bandwidths (8  $\mu\text{s}$ , 90° pulse). The residual proton peak of the solvent was suppressed by a 30- $\mu\text{s}$  presaturation pulse. The signal/noise was improved by exponential apodization

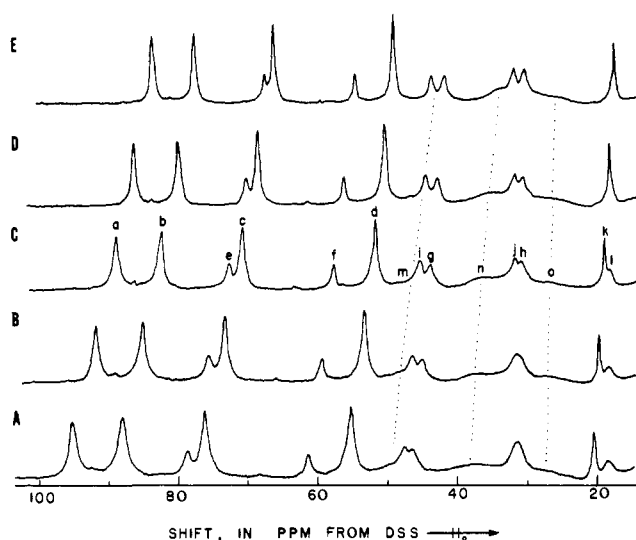


**Figure 1.** 360-MHz  $^1\text{H}$  NMR traces of the region 15–100 ppm downfield from DSS for 2 mM metMb $^2\text{H}_2\text{O}$  in 0.2 M NaCl $^2\text{H}_2\text{O}$  (p $^2\text{H}$  6.2) at (A) 15, (B) 25, (C) 35, (D) 45, and (E) 55 °C. The dotted lines follow the temperature dependence of the three broad resonances, m, n, and o.

which introduced 20-Hz line broadening; this inconsequentially affected resolution inasmuch as most isotropically shifted resonances have natural line widths  $\geq 300$  Hz. The probe temperature was calibrated by methanol. All chemical shifts are referenced to internal 2,2-dimethyl-2-silapentane-5-sulfonate (DSS) as internal calibrant; downfield shifts are defined as positive. Shifts are given at 25 °C unless noted otherwise. The pH was measured with a Beckman Model 3500 pH meter equipped with an Ingold microcombination electrode. The values are uncorrected for isotope effects and are referred to as p $^2\text{H}$ .

## Results

The low-field portion of the 360-MHz  $^1\text{H}$  NMR traces of metMb $^2\text{H}_2\text{O}$  at various temperatures are illustrated in Figure 1. Raising the temperature improves resolutions both by narrowing lines and due to differential temperature coefficients for the individual isotropic shifts (vide infra). Four obvious peaks of area 3 protons, a–d, and eight relatively narrow single proton peaks, e–l, are clearly resolved. Less obvious are at least three very broad resonances, m–o, in the region 25–40 ppm; m and o are probably single proton resonances, while n is consistent with containing two protons. Three single-proton peaks near 10 ppm are not shown ( $y_1$ ,  $y_2$ , and  $y_3$  in Table I).

The upfield region of the 360-MHz spectra is less temperature sensitive, and traces of metMb $^2\text{H}_2\text{O}$  at 25 and 45 °C are illustrated in A and B of Figure 2. The clearly resolved resonances t, u, and v correspond to 3, 3, and 2 protons, respectively (both the horizontal and vertical scales differ between Figures 1 and 2). At 55 °C, peak u actually splits into two single-proton peaks (inset in B of Figure 2).

In Figure 3 we compare the downfield portion of the 200-MHz  $^1\text{H}$  NMR traces of native metMb $^2\text{H}_2\text{O}$  (A) with that of metMb $^2\text{H}_2\text{O}$  reconstituted with [1,3-( $\text{C}^2\text{H}_3$ ) $_2$ ]hemin<sup>36</sup> (B) and 1,5-( $\text{C}^2\text{H}_3$ ) $_2$ ]hemin (C). The decreased intensity of peak d in both B and C confirms the identity of 1- $\text{CH}_3$ , while the presence of peak a in both B and C assigns 8- $\text{CH}_3$ . The unique decrease in intensity of peak c in B and peak b in C provides the remaining individual methyl assignments. Since the narrowest resonance, k, in Figures 1 or 2 also exhibits diminished intensity in the downfield trace of [1,3-( $\text{C}^2\text{H}_3$ ) $_2$ ]hemin-metMb $^2\text{H}_2\text{O}$  (B in Figure 3), where 6,7- $\text{H}_\beta$ 's are also partially deuterated,<sup>36</sup> it must arise from one of the four propionic acid  $\text{H}_\beta$ 's. The other three such resonances are not resolved.

Assignment of single-proton residues was carried out optimally at 45 °C and 360 MHz, where resonances are narrower.

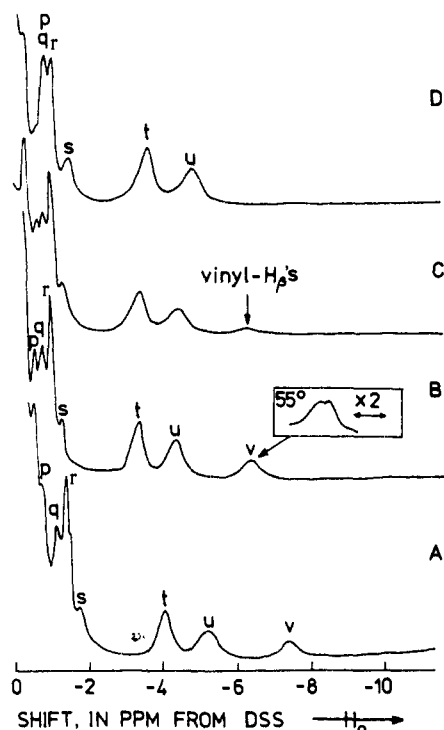


**Figure 2.** 360-MHz  $^1\text{H}$  NMR traces of the region 0–10 ppm upfield of DSS, of 2 mM protein solutions in 0.2 M NaCl in  $^2\text{H}_2\text{O}$ , at p $^{\text{H}}$  6.2 of (A) metMb $^2\text{H}_2\text{O}$  at 25  $^{\circ}\text{C}$ ; (B) metMb $^2\text{H}_2\text{O}$  at 45  $^{\circ}\text{C}$  (the inset is peak v at 55  $^{\circ}\text{C}$ ); (C) metMb $^2\text{H}_2\text{O}$  reconstituted with [2,4-( $^2\text{H}_\beta$ ) $_4$ ]hemin at 45  $^{\circ}\text{C}$ ; (D) deut-metMb $^2\text{H}_2\text{O}$  at 45  $^{\circ}\text{C}$ . The peaks with diminished intensity due to deuteration are indicated by arrows.

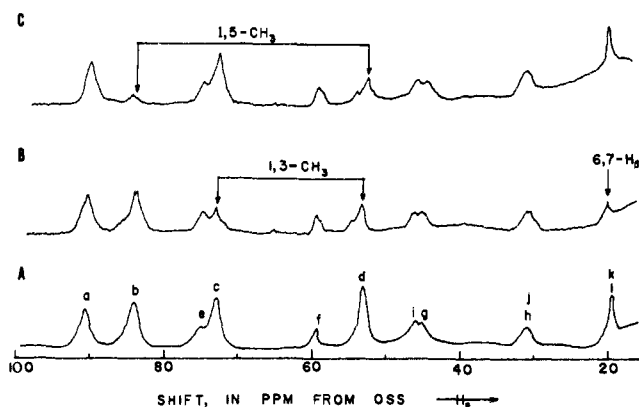


**Figure 3.** 200-MHz  $^1\text{H}$  NMR traces of the region 15–100 ppm downfield from DSS, at 27  $^{\circ}\text{C}$  and p $^{\text{H}}$  6.2 of (A) metMb $^2\text{H}_2\text{O}$  in 0.2 M NaCl in  $^2\text{H}_2\text{O}$ ; (B) metMb $^2\text{H}_2\text{O}$  reconstituted with [1,3-( $^2\text{C}^2\text{H}_3$ ) $_2$ ]hemin (also  $\sim$ 80% deuterated at 6,7- $\text{H}_\beta$ 's) in 0.2 M NaCl in  $^2\text{H}_2\text{O}$ ; (C) metMb $^2\text{H}_2\text{O}$  reconstituted with [1,5-( $^2\text{C}^2\text{H}_3$ ) $_2$ ]hemin, in 0.2 M NaCl in  $^2\text{H}_2\text{O}$ . The peaks with reduced intensity due to deuteration are indicated by arrows.

A in Figure 4 gives the trace of native metMb $^2\text{H}_2\text{O}$  at 45  $^{\circ}\text{C}$ , to be compared with that of [2,4-( $^2\text{H}_\alpha$ ) $_2$ ]hemin-reconstituted metMb $^2\text{H}_2\text{O}$  (B) and [*meso*-( $^2\text{H}$ ) $_4$ ]hemin-reconstituted metMb $^2\text{H}_2\text{O}$  (C). Both i and j disappear in trace B, clearly identifying them as vinyl  $\text{H}_\alpha$ 's. In trace C, the broad resonances in the region 25–50 ppm, particularly n and o, are significantly reduced in intensity, indicating that at least the latter two are meso  $\text{H}$ 's.

Comparison of the 360-MHz  $^1\text{H}$  NMR traces at 45  $^{\circ}\text{C}$  of native metMb $^2\text{H}_2\text{O}$  with that of metMb $^2\text{H}_2\text{O}$  reconstituted with [2,4-( $^2\text{H}_\beta$ ) $_4$ ]hemin reveals differences only in the upfield portions, as illustrated in B and C of Figure 2, where the two components of v must be vinyl  $\text{H}_\beta$  resonances. The other two  $\text{H}_\beta$  peaks are not resolved.

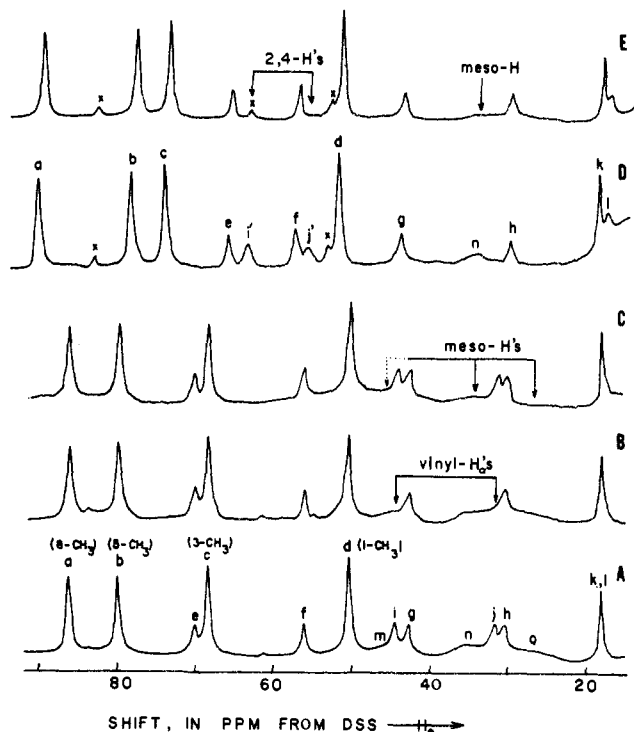


**Figure 4.** 360-MHz  $^1\text{H}$  NMR traces of the region 15–90 ppm downfield from DSS of 2 mM protein solutions in 0.2 M NaCl in  $^2\text{H}_2\text{O}$ , 45  $^{\circ}\text{C}$  and p $^{\text{H}}$  6.2 of (A) metMb $^2\text{H}_2\text{O}$ ; (B) metMb $^2\text{H}_2\text{O}$  reconstituted with [2,4-( $^2\text{H}_\alpha$ ) $_2$ ]hemin; (C) metMb $^2\text{H}_2\text{O}$  reconstituted with [*meso*-( $^2\text{H}$ ) $_4$ ]hemin; (D) deut-metMb $^2\text{H}_2\text{O}$ ; (E) deut-metMb $^2\text{H}_2\text{O}$  reconstituted with [2,4-( $^2\text{H}$ ) $_2$ ]deuterohemin (which also has some deuteration of meso  $\text{H}$ 's). The peaks with diminished intensities due to deuteration are indicated by arrows. The peaks in D and E marked by x probably arise from a minor component of deut-metMb $^2\text{H}_2\text{O}$  which has the porphyrin rotated 180 $^{\circ}$  about the  $\alpha$ - $\gamma$ -meso positions.

The high-field and low-field portions of the 360-MHz proton traces at 45  $^{\circ}\text{C}$  of deuterohemin-reconstituted metMb $^2\text{H}_2\text{O}$  (deut-metMb $^2\text{H}_2\text{O}$ ) are shown in D of Figures 2 and 4, respectively. The low-field trace of deut-metMb $^2\text{H}_2\text{O}$  reconstituted with [2,4-( $^2\text{H}$ ) $_2$ ]deuterohemin is shown in E of Figure 4. The upfield trace confirms the assignment of v to vinyl  $\text{H}_\beta$ 's, but otherwise does not differ significantly from that of metMb $^2\text{H}_2\text{O}$ . The downfield portion (D and E of Figure 4) again yields four methyl peaks, a–d. Two of the narrow single-proton peaks in the region 30–50 ppm are missing (vinyl  $\text{H}_\alpha$ 's), but two broader single-proton peaks appear near 60 ppm, i' and j' (D of Figure 4), which disappear in E of Figure 4. Hence peaks i' and j' clearly arise from the pyrrole 2,4- $\text{H}$ 's. The shifts, relative to DSS at 25  $^{\circ}\text{C}$ , for both proteins are listed in Table I.

The temperature dependence of the resolved isotropically shifted resonances, referenced to DSS, for metMb $^2\text{H}_2\text{O}$  at p $^{\text{H}}$  6.2 is exhibited in Figure 5 in the form of a Curie plot.<sup>16,17</sup> The apparent intercepts at  $T^{-1} = 0$  for the observed straight lines are given in parentheses on the left.

## Discussion

**Heme Resonance Assignments.** The isotope labeling in metMb $^2\text{H}_2\text{O}$  clearly assigns the individual methyl groups and identifies the two vinyl  $\text{H}_\alpha$ 's (i and j), two of the four vinyl  $\text{H}_\beta$ 's (u), and one of the four propionic acid  $\text{H}_\beta$ 's (e). The other vinyl  $\text{H}_\beta$ 's and propionic acid  $\text{H}_\beta$ 's (k) are unresolved in the diamagnetic envelope –1 to 10 ppm from DSS. The vinyl  $\text{H}_\beta$ 's are known to occur in pairs of resonances of unequal widths,<sup>17</sup> with the  $\text{H}_\beta$ (trans) peaks  $\sim$ 30% wider owing to their closer proximity to the iron. The relative width of the vinyl  $\text{H}_\beta$  and methyl resonances in model compounds<sup>17</sup> suggests that the resolved

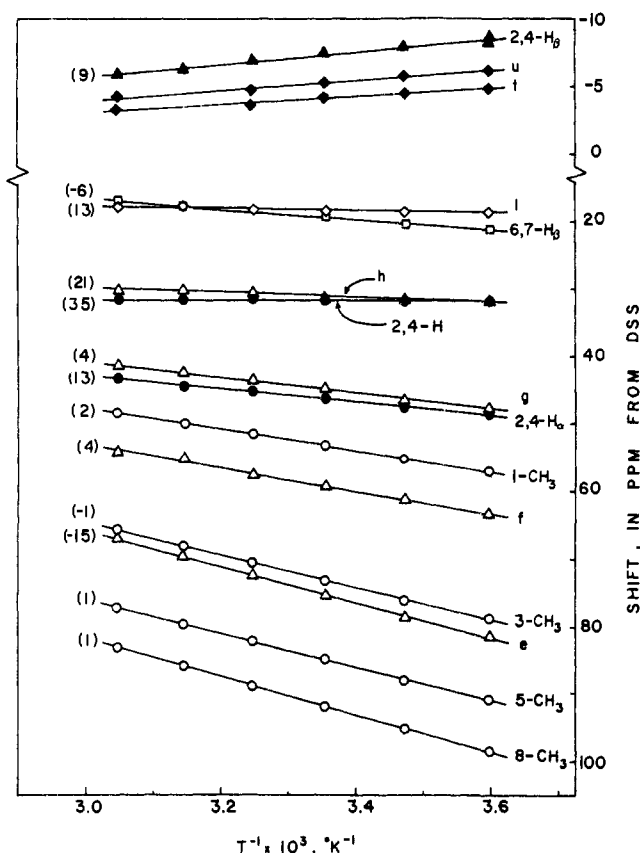


**Figure 5.** Curie plot for the resolved isotropically shifted resonances of metMb<sup>2</sup>H<sub>2</sub>O. If assigned unambiguously, the peaks are designated by their position in the porphyrin, A; otherwise the designations for peaks in C of Figure 1 are used. The apparent intercepts at  $T^{-1} = 0$  are given in parentheses on the left; the uncertainties are  $\pm 3$  ppm. The diamagnetic positions, in ppm (anticipated intercepts at  $T^{-1} = 0$ ), for the various functional groups are as follows: 1,3,5,8-CH<sub>3</sub>, 3.6; 6,7-H <sub>$\alpha$</sub> , 4.50; 6,7-H <sub>$\beta$</sub> , 3.40; 2,4-H <sub>$\alpha$</sub> (vinyl), 8.60; 2,4-H <sub>$\beta$</sub> (trans), 6.30 (La Mar, G. N.; Viscio, D. B.; Smith, K. M.; Caughey, W. S.; Smith, M. L. *J. Am. Chem. Soc.* **1978**, *100*, 8085-8092).

peaks in the protein (u) arise from H <sub>$\beta$</sub> (trans). This is also consistent with the H <sub>$\beta$</sub> (trans) resonating upfield of H <sub>$\beta$</sub> (cis) in models.<sup>17</sup>

The two H <sub>$\alpha$</sub> 's cannot be attributed unambiguously to individual vinyls, although a reasonable tentative assignment is proposed. Since 1-CH<sub>3</sub> has a much smaller isotropic shift than 3-CH<sub>3</sub>, pyrrole I must receive less unpaired spin density. On this premise, we expect 2-vinyl to exhibit smaller shifts than 4-vinyl, leading to the assignment of i to 4-vinyl and j to 2-vinyl.

The decrease in the areas of the broad peaks m, n, and o, particularly n and o, upon deuterating the meso-H's  $\sim 80\%$  (compare A and D of Figure 4) indicates that at least three of the meso-H peaks occur in the region 25-50 ppm from DSS. A similar decrease of the intensity of broad peaks in this area is noted on partial deuteration of the meso positions of deuterated metMb<sup>2</sup>H<sub>2</sub>O (i.e., compare D and E of Figure 4).

The four unassigned single proton peaks e-h of comparable line widths most likely arise from the four propionic acid H <sub>$\alpha$</sub> 's, based on the appearance of similar peaks in this region in model compounds.<sup>15,17,30</sup> A fifth, slightly broader unassigned single proton peak l, found  $\sim 20$  ppm below DSS, could also be a H <sub>$\alpha$</sub> , or could arise from the protein (vide infra). Definitive assignments of the H <sub>$\alpha$</sub> 's must await development of a convenient synthetic route to specific deuteration of each propionic side chain position.

The proton traces for native metMb<sup>2</sup>H<sub>2</sub>O and deuterated metMb<sup>2</sup>H<sub>2</sub>O (D and E of Figure 4) differ inconsequentially

**Table I.** Chemical Shifts for Resolved Resonances in Met-Aquo Myoglobins<sup>a</sup>

		metMb <sup>2</sup> H <sub>2</sub> O	deut-metMb <sup>2</sup> H <sub>2</sub> O		
methyl	{ 8 (a) 5 (b) 3 (c) 1 (d) e f g h	91.7 ( $\sim 300$ ) <sup>b</sup>	97.0 ( $\sim 300$ )		
		84.9	83.7		
		73.2	79.2		
		53.2	55.7		
		75.5 ( $\sim 250$ )	71.6 (250)		
		59.2	61.2		
		44.9	46.5		
		30.9	30.6		
		vinyl H <sub><math>\alpha</math></sub>	{ (i) (j)		
				46.4	
pyrrole 2,4-H	{ i' j'		68.2 (350)		
			60.3		
6,7-H <sub><math>\beta</math></sub>	{ (k) l	19.56 (140)	20.17		
		18.1 (400)	17.8		
meso H	{ (m) (n) (o)	$\sim 48$	<sup>c</sup>		
		37.4	$\sim 37$		
		$\sim 27$	<sup>c</sup>		
	y <sub>1</sub> , y <sub>2</sub> , y <sub>3</sub> <sup>d</sup>	10.25, 9.67, 9.11	10.44, 9.76, 9.13		
	p	-0.80	-0.74		
	q	-1.17	-1.21		
	r	-1.45	-1.47		
	s	-1.81	-1.82		
	t	-4.11 (110)	-4.13		
	u	-5.24 (200)	-5.28		
vinyl H <sub><math>\beta</math></sub>	(v) <sup>e</sup>	-7.43			

<sup>a</sup> Shifts in parts per million at 360 MHz, 25 °C, and referenced to internal DSS. <sup>b</sup> Line width in hertz at 360 MHz, given in parentheses. <sup>c</sup> Other meso H not clearly resolved. <sup>d</sup> Splits into two signals at 55 °C. <sup>e</sup> Three single-proton resonances which exhibit weak Curie behavior (line width  $\sim 50$  Hz).

except for the absence of vinyl peaks and the new 2,4-H's (peaks i' and j'). The spectra were also found to be similar in the metMbCN forms.<sup>18,19,38</sup> The known presence of a 5% component which has the heme rotated 180° about the  $\alpha$ - $\gamma$  meso axis<sup>19,39</sup> is probably responsible for three minor peaks marked x; the fourth peak is probably under methyl c, as suggested by area.

The NMR spectrum of metMbH<sub>2</sub>O thus yields 12 assigned (four methyls, three meso-H, four vinyl, one propionic acid H <sub>$\beta$</sub> ) peaks and 5 probable (four propionic acid H <sub>$\alpha$</sub> 's and the fourth meso H) resolved heme resonances out of a total of 22. In the case of low-spin metMbCN, only six assigned<sup>18</sup> (three methyl, three vinyl) and three probable (two propionic acid H <sub>$\alpha$</sub> 's, one meso H) are resolved at the same field strength. Thus the resolution and likely information content of high-spin met hemoproteins can be expected to be at least as high as that of the more frequently studied low-spin ferrics.

**Protein Peak Assignments.** In the absence of the ability to deuterate specific residues of the protein, assignments must rely on more indirect, and hence necessarily less definite, methods.

We have shown<sup>40</sup> elsewhere that a single-proton resonance observed in H<sub>2</sub>O solution is missing in the NMR spectrum of metMb<sup>2</sup>H<sub>2</sub>O in <sup>2</sup>H<sub>2</sub>O. The large 102-ppm downfield shift at 25 °C for this exchangeable proton requires that it originate from the proximal histidyl imidazole N<sub>1</sub>H. This same histidine peak has been assigned previously in metMbCN<sup>41</sup> and deoxy-Mb.<sup>42</sup>

The most likely origin of the one (possible more) nonexchangeable single-proton downfield peak which does not arise from the propionic acid H <sub>$\alpha$</sub> 's is one of the diastereotopic methylene protons of the proximal histidyl imidazole. These protons occupy a position relative to the iron similar to that of the propionic acid H <sub>$\alpha$</sub> 's, and hence should exhibit similar line widths, as found in models.<sup>43</sup>

The other resolved isotropically shifted peaks which cannot arise from the heme occur upfield of DSS (Figure 2). The peaks t and u consist of three protons each and remain single resonances in the range 5–55 °C, strongly supporting their assignment to methyl groups. The other partially resolved peaks p–s are consistent with one or two protons. The proximal histidine can be eliminated as a source of peaks p–s because of their small widths and the expectation that downfield  $\sigma$  contact shifts would dominate.<sup>15,17,42,44</sup> Thus the probable origins of these peaks are distal residues.<sup>10</sup>

Studies on models have shown<sup>16</sup> that high-spin ferric systems exhibit small downfield heme dipolar shifts due to zero-field splitting,<sup>37</sup> and that these dipolar contributions, varying as  $T^{-2}$ , impart curvature and nonzero intercepts to the Curie plots. The Curie plot in Figure 5 yields intercepts at  $T^{-1} = 0$  for the four methyls that are within 2–5 ppm of the diamagnetic position, indicating that the dipolar shifts are probably smaller than in the models, although in the same direction. Hence this predicts upfield dipolar shifts for distal residues near the iron.

The two distal residues<sup>10</sup> closest to the iron are valine E11 and histidine E7. One of the methyls of valine E11 is only 5.5 Å from the iron, so that the combination of upfield ring current and dipolar shifts as well as the large line width could account for peak u. The second valine E11 methyl is further from the iron, leading to smaller upfield shifts and line broadening, and most likely gives rise to peak t. The smaller, narrower peaks in the region 0 to –2 ppm could arise from his E7. Comparison of the upfield resonances in ferric hemoproteins possessing other distal residues may provide further support for some of these tentative assignments.

**Occupation of the Sixth Site.** Although the presence of a coordinated water is definitely established for met-myoglobins<sup>10</sup> and some met-hemoglobins,<sup>9</sup> and definitely eliminated for the monomeric met-hemoglobin from the *Chironomus* mosquito,<sup>45</sup> based on X-ray crystallographic investigations, considerable controversy exists over the state of ligation of other ferric hemoproteins such as the resting state of horseradish peroxidase.<sup>46,47</sup>

It has been shown<sup>15–17,30</sup> in high-spin ferric models that the NMR spectra of five- and six-coordinate complexes differ characteristically in two important aspects. The meso H's always appear upfield (~50 ppm) in five-coordinate models,<sup>15–17,30</sup> while the same peak is found downfield (~40 ppm) in six-coordinate complexes.<sup>15,17</sup> Moreover, while the methyl and pyrrole-proton (deut-metMb<sup>2</sup>H<sub>2</sub>O) peaks overlap in six-coordinate models, the latter peaks are considerably downfield (~25 ppm) of the former peaks in the five-coordinate system.<sup>17</sup>

The observed positions for meso H's and 2,4-H's in metMb<sup>2</sup>H<sub>2</sub>O and deut-metMb<sup>2</sup>H<sub>2</sub>O both confirm the presence of the liganded water and resultant six coordination in solution. The ability to resolve and assign these resonances in the present case suggests that the heme isotropic shift patterns can be utilized to probe the coordination state of the sixth position in other met-hemoproteins.

**Protein Influence on the Heme.** As was found in the case of low-spin ferric hemoproteins,<sup>3,18,19</sup> the spread of the four heme methyl shifts is much larger in the protein environment than in models,<sup>17,20</sup> indicating that a large rhombic and in-plane asymmetry is induced due to heme-apoprotein interactions. However, although the magnitude of the methyl spread is significantly increased over the models,<sup>17</sup> the pattern (1,3,5,8, reading downfield) of the individual methyls, in contrast to the low-spin systems,<sup>3</sup> is the same as in the models. The decreased sensitivity of methyl shifts to the effect of a rhombic perturbation was also found in comparing high-spin and low-spin model complexes,<sup>17,20</sup> and can probably be attributed to the reduced sensitivity of  $\sigma$  vs.  $\pi$  spin density to peripheral perturbations.<sup>44</sup>

The assignment of the individual methyls has already permitted the demonstration<sup>29</sup> that the differential perturbation of the methyl shifts can be used to determine the vicinity in which substrate binding<sup>48</sup> takes place in the heme cavity of high-spin met-hemoproteins.

**Side-Chain Mobility.** The data in Figure 5 shows that the iron spin magnetization follows the Curie law reasonably closely,<sup>16,37</sup> since the four heme methyls yield straight lines with intercepts at  $T^{-1} = 0$  very close to the diamagnetic methyl positions. The two vinyl H <sub>$\alpha$</sub>  shifts (peaks i and j), however, both deviate from the Curie law so as to decrease slower with  $T^{-1}$  than predicted, with the deviations much larger for i than j, the proposed 4-vinyl and 2-vinyl peaks, respectively.

Similar deviations for vinyl H <sub>$\alpha$</sub> 's were observed in model compounds of both high-spin<sup>17</sup> and low-spin iron,<sup>23</sup> and attributed to the oscillatory mobility of the vinyls. Thus the deviations from the Curie law arise from the change in the average orientation of the vinyl from more out of plane with small  $\pi$  contact shifts at low temperature (sterically favored) to more in plane with large  $\pi$  contact shifts at higher temperature.<sup>23</sup> Since the nonzero intercept is much larger for j than i, the former must be more mobile or have less repulsive interactions with the proteins to keep it out of plane. X-ray data<sup>10</sup> show that the specific steric interactions involve threonine C4 with 4-vinyl and phenylalanine H15 with 2-vinyl. The crystal data also show that Phe H15 is readily displaced from the heme by binding xenon<sup>48</sup> or the mercuric triiodide anion<sup>49</sup> in the heme cavity. This suggests that 2-vinyl should be more mobile, which agrees with our tentative assignments of the vinyl H <sub>$\alpha$</sub> 's for j to 2-vinyl.

Of the four proposed propionic acid H <sub>$\beta$</sub> 's, e–h, two follow the Curie law (f and g), while two deviate significantly, e decreasing much faster (intercept –15 ppm), while h decreases much slower (intercept 21 ppm) than  $T^{-1}$ . Such temperature-dependent coupling constants are characteristic for oscillatory mobile  $\alpha$ -methylene protons.<sup>23,50</sup> Since both protons of an  $\alpha$ -CH<sub>2</sub> must deviate if the CH<sub>2</sub> orientation changes, f, g and e, k probably belong to the mobile and the "locked" propionic acid side chains, respectively.

The crystal structure of metMbH<sub>2</sub>O shows<sup>10</sup> both propionic acids involved in two hydrogen-bonding interactions, though one of the interactions involving 7-propionic acid is to another metMbH<sub>2</sub>O in the crystal. This may suggest that in solution it is this propionic acid which is more mobile. Again, a more quantitative discussion must await the unambiguous assignments of all H <sub>$\alpha$</sub> 's. However, the present data clearly demonstrate the potential for utilizing differential deviations from Curie behavior for providing information on the stability and structural integrity of hydrogen-bonding interaction between the heme and apoprotein in solution.

**Acknowledgments.** The authors are indebted to J. de Ropp and N. L. Davis for reconstituting some of the myoglobins. This research was supported by grants from the National Institutes of Health, HL-16087 and HL-22252, and the University of California, Davis, NMR Facility.

## References and Notes

- Wüthrich, K. *Struct. Bonding (Berlin)* **1970**, *8*, 53–121.
- Morrow, J. S.; Gurd, F. R. N. *CRC Crit. Rev. Biochem.* **1975**, *3*, 221–287.
- La Mar, G. N. In "Biological Applications of Magnetic Resonance," Shulman, R. G., Ed.; Academic Press: New York, 1979; pp 305–343.
- Antonini, E.; Brunori, M. "Hemoglobin and Myoglobins in Their Reactions with Ligands"; North-Holland Publishing Co.: Amsterdam, 1971.
- Kurland, R. J.; Davis, D. G.; Ho, C. *J. Am. Chem. Soc.* **1968**, *90*, 2700–2701.
- Morishima, I.; Ogawa, S.; Inubushi, T.; Iizuka, T. *Adv. Biophys.* **1978**, *11*, 217–245.
- McGrath, T. M.; La Mar, G. N. *Biochim. Biophys. Acta* **1978**, *534*, 99–111.
- Perutz, M. F.; Heidner, E. J.; Ladner, J. E.; Bettlestone, J. G.; Ho, C.; Slade, E. F. *Biochemistry* **1974**, *13*, 2187–2200.

- (9) Perutz, M. F. *Br. Med. Bull.* **1976**, *32*, 195–208.  
 (10) Takano, T. *J. Mol. Biol.* **1977**, *110*, 537–568.  
 (11) Yamazaki, I. In "Molecular Mechanisms of Oxygen Activation", Hayaishi, O., Ed.; Academic Press: New York, 1974; pp 535–558.  
 (12) Saunders, B. C. In "Inorganic Biochemistry", Eichhorn, G. I., Ed.; Elsevier: Amsterdam, 1973; Vol. 2, pp 988–1021.  
 (13) Gunsalus, I. C.; Meeks, J. R.; Lipscomb, J. D.; Debrunner, P.; Münck, E. M. In ref 11, pp 559–613.  
 (14) Bartsch, R. G. In "The Photosynthetic Bacteria", Clayton, R. K., Siström, W. R., Eds.; Plenum Press: New York, in press.  
 (15) Kurland, R. J.; Little, R. G.; Davis, D. G.; Ho, C. *Biochemistry* **1971**, *10*, 2237–2246.  
 (16) La Mar, G. N.; Eaton, G. R.; Holm, R. H.; Walker, F. A. *J. Am. Chem. Soc.* **1973**, *95*, 63–75.  
 (17) Budd, D. L.; La Mar, G. N.; Langry, K. C.; Smith, K. M.; Nayyir-Mazhir, R. *J. Am. Chem. Soc.* **1979**, *101*, 6091–6096.  
 (18) Mayer, A.; Ogawa, S.; Shulman, R. G.; Yamane, T.; Cavaleiro, J. A. S.; Rocha Gonsalves, A. M. d'A.; Kenner, G. W.; Smith, K. M. *J. Mol. Biol.* **1974**, *86*, 749–756.  
 (19) La Mar, G. N.; Budd, D. L.; Viscio, D. B.; Smith, K. M.; Langry, K. C. *Proc. Natl. Acad. Sci. U.S.A.* **1978**, *75*, 5755–5759.  
 (20) La Mar, G. N.; Viscio, D. B.; Smith, K. M.; Coughney, W. S.; Smith, M. L. *J. Am. Chem. Soc.* **1978**, *100*, 8085–9092.  
 (21) Morishima, I.; Iizuka, T. *Biochim. Biophys. Acta* **1975**, *386*, 542–555.  
 (22) La Mar, G. N.; Overkamp, M.; Sick, H.; Gersonde, K. *Biochemistry* **1978**, *17*, 352–361.  
 (23) La Mar, G. N.; Viscio, D. B.; Gersonde, K.; Sick, H. *Biochemistry* **1978**, *17*, 361–367.  
 (24) La Mar, G. N.; Budd, D. L.; Sick, H.; Gersonde, K. *Biochim. Biophys. Acta* **1978**, *537*, 270–283.  
 (25) Norvell, J. C.; Nunes, A. C.; Schoenborn, B. P. *Science* **1975**, *190*, 568–570.  
 (26) Takano, T. *J. Mol. Biol.* **1977**, *110*, 569–584.  
 (27) Dunford, H. B., submitted for publication in *Adv. Inorg. Chem.*  
 (28) Morishima, I.; Ogawa, S. *J. Biol. Chem.* **1979**, *254*, 2814–2820.  
 (29) La Mar, G. N.; Budd, D. L. *Biochim. Biophys. Acta* **1979**, *581*, 201–209.  
 (30) Johnson, L. F.; Coughney, W. S. *Chem. Commun.* **1969**, 1362–1364.  
 (31) Falk, J. E. "Porphyrins and Metalloporphyrins"; Elsevier: Amsterdam, 1964; p 179.  
 (32) Kenner, G. W.; Smith, K. M.; Sutton, M. J. *Tetrahedron Lett.* **1973**, 1303–1306.  
 (33) Führop, J. H.; Smith, K. M. In "Porphyrins and Metalloporphyrins", Smith, K. M., Ed.; Elsevier: Amsterdam, 1975; p 803.  
 (34) Kenner, G. W.; Quirke, J. M. E.; Smith, K. M. *Tetrahedron* **1976**, *32*, 2753–2756.  
 (35) Teale, F. W. J. *Biochim. Biophys. Acta* **1959**, *35*, 543.  
 (36) The method for introducing deuterium into methyl-1 and -3 (Evans, B.; Smith, K. M.; La Mar, G. N.; Viscio, D. B. *J. Am. Chem. Soc.* **1977**, *99*, 7070–7072) also introduces extensive deuteration of the 6,7-propionic acid H<sub>β</sub>'s.  
 (37) Jesson, J. P. In "NMR of Paramagnetic Molecules", La Mar, G. N., Horrocks, Jr., W. D., Holm, R. H., Eds.; Academic Press: New York, 1973; pp 1–52.  
 (38) Shulman, R. G.; Wüthrich, K.; Yamane, T.; Antonini, E.; Brunori, M. *Proc. Natl. Acad. Sci. U.S.A.* **1969**, *63*, 623–628.  
 (39) La Mar, G. N.; Budd, D. L.; Davis, N. L., results to be published.  
 (40) La Mar, G. N.; de Ropp, J. S. *Biochem. Biophys. Res. Commun.* **1979**, *90*, 36–41.  
 (41) Sheard, B.; Yamane, T.; Shulman, R. G. *J. Mol. Biol.* **1970**, *53*, 35–48.  
 (42) La Mar, G. N.; Budd, D. L.; Goff, H. *Biochem. Biophys. Res. Commun.* **1977**, *77*, 104–110.  
 (43) La Mar, G. N.; Satterlee, J. D.; Frye, J. S. *Biochim. Biophys. Acta* **1976**, *428*, 78–90.  
 (44) La Mar, G. N.; Walker-Jensen, F. A. In "The Porphyrins", Dolphin, D., Ed.; Academic Press: New York, 1978; Vol. IVC, pp 61–157.  
 (45) Steigemann, W.; Weber, E. *J. Mol. Biol.* **1979**, *127*, 309–338.  
 (46) Lanir, A.; Schejter, A. *Biochem. Biophys. Res. Commun.* **1975**, *62*, 199–203.  
 (47) Vuk-Pavlovic, S.; Benko, B. *Biochem. Biophys. Res. Commun.* **1975**, *66*, 1154–1159.  
 (48) Schoenborn, B. P.; Watson, H. C.; Kendrew, J. C. *Nature (London)* **1965**, *207*, 28–30. Schoenborn, B. P. *ibid.*, **1967**, *214*, 1120–1122.  
 (49) Kretsinger, R. H.; Watson, H. C.; Kendrew, J. C. *J. Mol. Biol.* **1966**, *31*, 305–314.  
 (50) La Mar, G. N. In ref 37, pp 85–126.

## X-ray and NMR Studies of L-4-Hydroxyproline Conformation in Oligopeptides Related to Collagen

Christiane Garbay-Jaureguiberry,<sup>1a</sup> Bernadette Arnoux,<sup>1b</sup> Thierry Prangé,<sup>\*1b</sup> Suzanne Wehri-Altenburger,<sup>1a</sup> Claudine Pascard,<sup>1b</sup> and Bernard P. Roques<sup>\*1a</sup>

Contribution from the Département de Chimie Organique, UER des Sciences Pharmaceutiques et Biologiques, 75006 Paris, France, and Cristalochimie, Institut de Chimie des Substances Naturelles, C.N.R.S., 91190 Gif sur Yvette, France. Received February 5, 1979

**Abstract:** Correlative solid/solvated state analyses of some L-4-hydroxyproline containing oligopeptides, mainly Gly-L-4Hyp, L-Pro-L-4Hyp, *cyclo*-(L-Pro-L-4Hyp), and *N*-Ac-L-Pro-L-4Hyp, have been undertaken by use of X-ray (single crystal) and NMR techniques (solution). The main features deduced from these comparative analyses are as follows: (1) the rapid conformational flexibility of C<sup>γ</sup> of L-Pro residues is largely inhibited in L-4Hyp, leading to a much more rigid structure in solution and in the crystal; (2) L-4Hyp rings are much more puckered than L-Pro; (3) the same dynamic deformations of the rings are derived from X-ray  $\langle B \rangle$  thermal parameters compared to the carbon-13  $NT_1$  factors, despite different *cis/trans* isomerism around amide bonds. Very similar conformations are observed by both methods. This gives additional evidence for the key role played by the L-4Hyp residues in the stability of triple helical peptides related to collagen.

### Introduction

Many studies have been performed to understand the structural role of the pyrrolidine residues L-Pro and L-4Hyp in collagen.<sup>2,3</sup> This polypeptide contains a great number of repeated Gly-L-Pro-L-4Hyp tripeptide sequences and experimental evidence has shown that Hyp residues contribute to the stability of the triple helical structure.<sup>2b,3</sup> On the other hand, recent studies<sup>4</sup> suggest that the *cis* ⇌ *trans* isomerism around the X-L-Pro peptide bond could be involved in the folding of proteins.

Both synthetic peptides (L-Pro-L-Pro-Gly)<sub>n</sub> and (L-Pro-L-4Hyp-Gly)<sub>n</sub>, *n* < 10, form triple-helical structures<sup>5–7</sup> and the role of L-4Hyp in stabilizing the triple helix was demonstrated by the higher thermal transition temperature of the

polymer containing L-4Hyp.<sup>5,6,8,9</sup> For Traub<sup>10</sup> and Ramachandran<sup>2a,3</sup> such an effect of L-4Hyp is due to participation of the γ OH group in additional hydrogen bonds between the chains via a water molecule. Evidence has been presented for the existence of intermolecular water bridges in poly(L-4Hyp)<sup>2,3,9,11</sup> and in the crystal of *N*-Ac-L-4Hyp.<sup>44</sup>

However, this proposed key role of L-4Hyp by specific interaction with a water molecule<sup>8</sup> in collagen and/or related peptides (L-Pro-L-Pro-Gly)<sub>n</sub> and (L-Pro-L-4Hyp-Gly)<sub>n</sub> may not fully account for a leading part in the triple-helix stabilization. As previously suggested,<sup>12,13</sup> when compared to L-Pro, the L-4Hyp residue seems to stabilize the helix by more subtle intrinsic effects (i.e., ring flexibility and restrictions of local backbone motion).